Theor Chem Acc (1998) 100:253–263
DOI 10.1007/s002149800m73

Theoretical
Chemistry Accounts

Regular article

Choosing GTO basis sets for periodic HF calculations*

Armin Grüneich, Bernd A. Heß

Institut für Physikalische und Theoretische Chemie, Universität Bonn, Wegelerstrasse 12, D-53115 Bonn, Germany

Received: 20 July 1998 /Accepted: 21 August 1998 / Published online: 19 October 1998

Abstract. We investigate numerical linear dependencies of Gaussian-type orbital basis sets employed in the framework of the Hartree-Fock self-consistent field method for periodic structures, which so far have hampered the use of extended basis sets for non-ionic crystals. These linear dependencies occur when diffuse basis functions are included in a basis set in an uncontrolled manner. We use the condition number of the overlap matrix to lead us in the construction of extended basis sets for periodic structures which avoid numerical linear dependencies. Extended basis sets of high quality are optimized for a number of periodic structures (fcc He, α-Be, α-BN, and B1 NaF) with respect to the energy of the constituent atoms or ions. The results obtained with our basis sets, which do not require reoptimization in the crystal environment, compare favorably with those obtained with other extended basis sets reported in the literature.

Key words: Periodic Hartree-Fock – Gaussian basis sets

1 Introduction

It is fairly well known how a basis set should be chosen for atoms and molecules to ensure acceptable convergence of a given property in an ab initio calculation with minimal computational effort. Much empirical knowledge has been acquired on the choice of basis sets [1, 2] in the decades since Boys suggested the use of Gaussian-type orbitals (GTOs) in 1950 [3], and much effort has been taken to understand basis set incompleteness effects in atoms and molecules on a practical [4–6] and theoretical [7–9] level. Thus the problem of choosing GTO basis sets for quantum chemical investigations of atoms and molecules is fairly well understood.

In this paper we are concerned with a different situation: the basis sets used for the computation of periodic structures in the framework of linear combination of atomic orbitals to crystal orbitals (LCAO-CO) Hartree-Fock (HF) theory. Minimal and small split-valence basis sets optimized for use in atomic and molecular calculations are frequently employed often after reoptimization for the solid-state system under investigation. Even moderately extended basis sets, however, tend to numerical linear dependencies when used in ab initio studies of periodic systems. Consequently in the case of crystal computations, basis sets of uniform quality for a whole class of atoms or hierarchies of basis sets of increasing quality for one atom are scarce and a considerable fraction of the calculations on periodic systems are undertaken with fairly limited basis sets [10–12]. So one is still [13] faced with a situation where even the somewhat more extended basis sets that were used in solid state HF-self consistent field (SCF) calculations, for example, in Refs. [14–17], are modest compared to those employed for molecular calculations, although the use of large basis sets is computationally feasible [18].

In Sect. 2 a strategy based on theoretical considerations is derived for the optimization of GTO basis sets for periodical systems. This strategy (or modification thereof) is then employed to obtain basis sets for (fcc) He, (hcp) α-Be, α-BN, and B1 NaF, which were treated using the CRYSTAL 92 suite of programs. The results of the calculations based on these basis sets are reported in Sect. 3. Finally our results are summarized and conclusions are drawn.

2 Theoretical considerations

In the periodic (LCAO-CO)-HF approach, Bloch functions $\Phi_\mu(\mathbf{r};\mathbf{k})$ are used which are the result of adapting spatially localized functions $\chi_\mu(\mathbf{r}-\mathbf{R}_\mu)$, centered at $\mathbf{R}_\mu = (X_\mu, Y_\mu, Z_\mu)$, to the translational symmetry of a crystal, which is modeled to be ideally periodic

$$\Phi_\mu(\mathbf{r};\mathbf{k}) = \sum_{\mathbf{g}} e^{i\mathbf{k}\cdot\mathbf{g}}\chi_\mu(\mathbf{r}-\mathbf{R}_\mu-\mathbf{g}). \quad (1)$$

The sum runs over all direct lattice vectors $\mathbf{g}$.

* Dedicated to Prof. Dr. Wilfried Meyer on the occasion of his 60th birthday

Correspondence to: B. Heß

For the sake of argument, we consider orthorhombic systems and choose the generating functions as tensorial products of functions of the cartesian components (e.g., as cartesian Gaussian functions). Then the Bloch functions themselves can be factored

$$\Phi_\mu(\mathbf{r};\mathbf{k}) = \sum_{g_x g_y g_z} e^{ik_x g_x} e^{ik_y g_y} e^{ik_z g_z} \chi_\mu(x - X_\mu - g_x) \times \chi_\mu(y - Y_\mu - g_y)\chi_\mu(z - Z_\mu - g_z) \quad (2)$$

$$= \phi_\mu(x;k_x)\phi_\mu(y;k_y)\phi_\mu(z;k_z). \quad (3)$$

Introducing the lattice parameters $T_i, i \in \{x,y,z\}$ and writing out the function of the x coordinate in Eq. (3) as an example, the components of the Bloch functions can be rewritten as

$$\phi_\mu(x;k_x) = \sum_{l\in Z} e^{ik_x l T_x} \chi_\mu(x - X_\mu - lT_x). \quad (4)$$

For components of the $\mathbf{k}$ vector that are rational multiples of $2\pi/T_x$, that is for $k_x = 2\pi\frac{m}{nT_x}$, it is possible to define a super cell, for which the phase factors $c(k_x,l) = \exp(2\pi i\frac{m}{n}l)$ form a periodic sequence in l with period n. Thus the 1D components of the Bloch function can be interpreted as complex linear combinations of the functions $\tilde{\chi}_\mu(x)$

$$\phi_\mu(x;k_x) = \sum_{l=0}^{n-1} c(k_x,l)\tilde{\chi}_\mu\left(x - X_\mu^l\right) \quad (5)$$

$$\tilde{\chi}_\mu(x) = \sum_{j\in Z} \chi_\mu(x - jT), \quad (6)$$

where $X_\mu^l = X_\mu + lT_x$, and $T = nT_x$ is the lattice parameter of the super cell, which is dependent on the particular $\mathbf{k}$ vector under consideration. The $\tilde{\chi}_\mu(x)$ are by construction periodic functions in x with period T and we refer to them as periodized GTOs (PGTOs).

2.1 Periodized GTO

The PGTOs $\tilde{\chi}_\mu$ defined according to Eq. (6) are superpositions of GTOs centered at the nodes of an infinite, regular grid with period T. Considering the simplest cases, we restrict the generating functions χ_μ to normalized 1D s- and p-type GTOs, which are centered at coordinate r in the reference cell (see Fig. 1)

$$\chi_s = \left(\frac{2\alpha}{\pi}\right)^{1/4} e^{-\alpha(x-r)^2} \quad (7)$$

$$\chi_p = 2\left(\frac{2\alpha^3}{\pi}\right)^{1/4} (x-r)e^{-\alpha(x-r)^2}. \quad (8)$$

Since the GTOs in neighboring cells have nonzero overlap, the PGTOs are in general not normalized, as can be seen from the squared norm of their Fourier expansion in the unit cell:

$$\langle\tilde{\chi}_s|\tilde{\chi}_s\rangle = \sqrt{\frac{2\pi}{T^2\alpha}} \sum_{n=-\infty}^{\infty} \exp\left(-\frac{2\pi^2 n^2}{T^2\alpha}\right) \quad (9)$$

$$\langle\tilde{\chi}_p|\tilde{\chi}_p\rangle = \frac{4}{T^3}\sqrt{\frac{2\pi^5}{\alpha^3}} \sum_{n=-\infty}^{\infty} n^2 \exp\left(-\frac{2\pi^2 n^2}{T^2\alpha}\right). \quad (10)$$

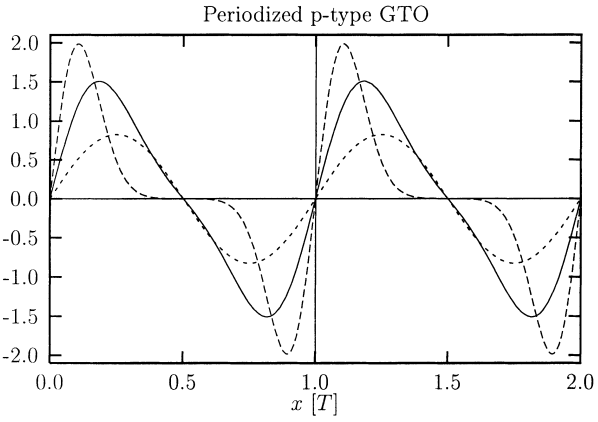

Fig. 1. Periodized *p-type GTO* for different exponents over the range of two lattice constants T

It is quite instructive to derive the limits of the sums [Eqs. (9) and (10)] for large and small exponents α,

$$\lim_{\alpha\to 0}\langle\tilde{\chi}_s|\tilde{\chi}_s\rangle = \infty \qquad \lim_{\alpha\to\infty}\langle\tilde{\chi}_s|\tilde{\chi}_s\rangle = 1 \quad (11)$$

$$\lim_{\alpha\to 0}\langle\tilde{\chi}_p|\tilde{\chi}_p\rangle = 0 \qquad \lim_{\alpha\to\infty}\langle\tilde{\chi}_p|\tilde{\chi}_p\rangle = 1. \quad (12)$$

This result is not surprising, since for large α the generating GTOs are isolated within the unit cell and their original normalization is retained in the PGTOs. For small exponents, the generating functions reach beyond the reference cell and hence are able to interfere (constructively for s-type GTOs and destructively for p-type GTOs) with their neighbors.

It is also quite instructive to consider the first Fourier coefficients of the *normalized* PGTO and their limits for small exponents. Denoting the kth mode by $|e_k\rangle = \exp(-2\pi i\frac{kx}{T})$, we have

$$\lim_{\alpha\to 0}|\langle e_0|\tilde{\chi}'_s\rangle|^2 = 1 - 2\exp\left(-\frac{2\pi^2}{\alpha T^2}\right) + O\left[\exp\left(-\frac{4\pi^2}{\alpha T^2}\right)\right] \quad (13)$$

$$\lim_{\alpha\to 0}|\langle e_1|\tilde{\chi}'_p\rangle|^2 = 1 - 4\exp\left(-\frac{6\pi^2}{\alpha T^2}\right) + O\left[\exp\left(-\frac{12\pi^2}{\alpha T^2}\right)\right]. \quad (14)$$

That is to say, periodized functions constructed from diffuse s- and p-type GTOs converge exponentially to the 0 and 1 mode of the Fourier expansion for small α. Consequently, two diffuse PGTOs located at the same center r have very similar overlap with their limit modes and thus easily become linearly dependent for small exponents.

In the course of a HF-SCF calculation one needs to orthonormalize the atomic orbital basis. In order to do this for a given set of PGTOs, one has to determine its overlap matrix $\mathbf{S}$, which can then be used to obtain the orthogonal PGTOs $\tilde{\chi}'_\mu$, for example, via symmetric orthogonalization, by solving the matrix equation

$$|\tilde{\chi}'_\mu\rangle = \mathbf{S}^{1/2}|\tilde{\chi}_\mu\rangle. \quad (15)$$

If this is done numerically, a small numerical error in the vector representation of $\tilde{\chi}_\mu$ will result in an error in $\tilde{\chi}'_\mu$, which is proportional to the condition number of the transformation matrix cond($\mathbf{S}^{1/2}$). We take cond($\mathbf{S}^{1/2}$) as the ratio of the largest and smallest eigenvalue of $\mathbf{S}^{1/2}$. It determines the numerical stability of the orthogonalization Eq. (15) (and hence of any SCF procedure that relies on such orthogonalization).

There are two factors that govern the condition number of the transformation matrix: the diffuseness and the number of the diffuse functions χ_μ included in the basis set. In the case of just one diffuse PGTO, one diagonal element of $\mathbf{S}$ will be large or small, depending on the angular momentum type of the basis function. This implies an unfavorable condition number of $\mathbf{S}$ and hence of $\mathbf{S}^{1/2}$. This situation is aggravated, if additional diffuse generating functions of the same angular momentum type are included in the basis set. In this case the absolute value of some off-diagonal elements and of some diagonal elements of $\mathbf{S}$ will be very similar. Upon diagonalization this will lead to a large splitting of the eigenvalues and hence to a bad condition number for $\mathbf{S}$. In practical calculations the number of diffuse basis functions is much more critical than their diffuseness.

The fact that diffuse basis functions lead to numerical instabilities can be understood from a physical reasoning. Diffuse GTOs are needed for atoms or molecules to describe electronic motion far away from the atomic center, like in a Rydberg state, for example. In a solid-state system, however, electrons cannot be far away from one nucleus without being close to another. Thus diffuse basis functions are needed in solid-state systems only to the extent that they allow polarization of the charge density between the nuclei. In order to include this polarization ability while avoiding numerical linear dependencies in solid-state calculations, it is vital to derive a measure for the diffuseness of a basis set.

The magnitude of the residual terms, i.e., the squared amplitudes of the higher than 0th (1st) modes in Eqs. (14) and (15) depend on the product αT^2. For a given exponent, the residual term decreases with smaller T, which is in turn dependent on the $\mathbf{k}$ value under consideration. (Higher values of $\mathbf{k}$ imply that the period T of the super cell is larger.) The smallest lattice constant T_Γ is realized for the high symmetry (Γ) point in $\mathbf{k}$ space; that is for $\mathbf{k} = 0$. This suggests measuring the exponent of a primitive GTO in multiples of T_Γ^{-2} and defining a generalization of the concept of even-tempered basis sets for solid-state calculations, with exponents α_i given by

$$\alpha_i = \frac{\gamma}{T_\Gamma^2}\beta^i \quad i = 0, 1, 2, \ldots \quad . \tag{16}$$

In this equation γ measures the diffuseness of the basis set and β is the ratio between two adjacent exponents. In a real (3D) system it is convenient to identify T_Γ with the nearest-neighbor separation. One can show that two basis sets chosen according to Eq. (16) for different lattice constants with given γ and β will lead to the same overlap matrix. It should be noted that scaling of GTO exponents with T^{-2} has previously been used to assure uniform convergence of the overlap matrix for different lattice constants in an HF-SCF calculation of diamond [19].

2.2 Strategies for the optimization of basis sets

Carefully choosing the parameters γ and β in Eq. (16) for an even-tempered basis guarantees a well-conditioned overlap matrix and hence numerical linear independence. In practice, subsequently optimizing and contracting such an even-tempered basis set does not alter the situation significantly, since the exponents do not change much in the course of optimization if they were reasonably chosen in the first place. In order to derive a suitable basis set for elementary solids, one should thus first obtain an even-tempered basis set according to Eq. (16) and subsequently optimize it.

First β and the number of primitive GTOs of one angular momentum type are determined, as desired ($\beta = 2.5 - 4.5$ would be a good choice, c.f. Ref. [4]). Then a guess is made at the initial value of the smallest exponent $\alpha_{\min}$ and a geometrical series of exponents is obtained $\alpha_i = \alpha_{\min}\beta^i$. The optimal value of $\gamma = \alpha_{\min}D^2$ can then be derived by monitoring the maximum condition number of the overlap matrix for this basis set at varying nearest-neighbor distances D for the crystal structure at hand (c.f. Sect. 3.2). Once β and γ are chosen in this way, a new set of exponents can be derived as an even-tempered series according to Eq. (16), where T_Γ is taken as the smallest expected nearest-neighbor separation.

The basis set thus obtained should be subsequently optimized for the isolated atom or ion, while the most diffuse exponent – the pivot – is held fixed. For that purpose it will be frequently necessary to augment the even-tempered basis set by an auxiliary primitive GTO that is more diffuse than the pivot. This will prevent the second most diffuse exponent from becoming smaller than the pivot in the course of the basis set optimization. Afterwards, the auxiliary primitive can either be removed from the basis or it can be contracted with one of the more compact GTOs. The same procedure can be applied to nonelementary solids, if for each element involved T_Γ is chosen as twice its covalent or ionic radius.

3 Results and Discussion

In order to check the optimization strategies derived in the previous section, basis sets were optimized for use in four test cases: a hypothetical fcc He crystal, α-Be, α-BN, and the B1 phase of NaF. The first system was chosen to demonstrate our ideas, while the remaining three systems reflect standard situations which occur in solid-state calculations: a metallic, a covalent, and an ionic system. Since the structure of α-BN is determined by a subtle balance of electrostatic attraction and Pauli repulsion, it serves as an example for covalent as well as for molecular solids which feature dispersion interactions.

3.1 Computational Details

All our basis sets were energy optimized for the isolated atoms or ions, using the TURBOMOLE 2.30 suite of programs with standard, i.e., default computational parameters as supplied. The subsequent solid-state cal-

culations were done with the CRYSTAL 92 suite of programs, with rather strict computational parameters: The threshold (ITOL) parameters which control the accuracy of the computation of the mono- and bielectronic Coulomb and exchange series were kept at the "very good" (cf. Ref. [20]) setting. In the case of B1-NaF they were even tightened to 8 10 8 10 17, in order to obtain a smooth potential curve. The Fock matrix was diagonalized at a sample of 93, 133, and 145 **k** points in the irreducible wedge of the Brillouin zone in the calculation of α-Be, α-BN, and B1-NaF, respectively. Usually a Fock matrix mixing of 30% was used to facilitate convergence of the SCF part of the calculations. For some calculations it was necessary to compile the CRYSTAL 92 programs with dimensional parameters exceeding the ones suggested for "large systems" in Ref. [20].

3.2 fcc Helium

In view of the the lack of dispersion interaction, we expect a purely repulsive potential curve for fcc He in the HF-SCF model. Thus spurious binding effects due to the basis set superposition error (BSSE) can be clearly identified.

A primitive 10*s* basis for He was fully optimized, starting from a geometrical series of exponents with $\alpha_{\min} = 0.01$, and a ratio of successive exponents $\beta = 3$. The optimized basis set was then contracted according to the scheme {511111} and augmented with two *p*-type polarization functions. The final basis set, as employed in our calculations, is listed in Table 1.

From this $(10s2p)/[6s2p]$ basis three smaller basis sets were derived by successive truncation of one, two, and three of the most diffuse primitive functions. We term these truncated basis sets $(9s2p)/[5s2p]$, $(8s2p)/[4s2p]$, and $(7s2p)/[3s2p]$. In Sect. 3.1 it was discussed that the condition number of the overlap matrix of an even-tempered basis set depends primarily on the ratio $\gamma = \alpha_{\min}/D^2$, with D the nearest-neighbor separation and $\alpha_{\min}$ the smallest exponent.

In Fig. 2 the maximum condition number of the overlap matrices **S(k)** for a sample of 29 **k** points is plotted over γ. From Fig. 2 it can be seen that the poles in the maximum condition number of the overlap matrices occur for all four basis sets for $\gamma \approx 3$. Choosing $\alpha_{\min}$ such that $\gamma \geq 6$ thus guarantees that numerical linear dependencies will be avoided. Note that the $(10s2p)/[6s2p]$ basis and its truncated derivatives are not even-tempered sets, since each exponent was individually optimized and the inner shell was contracted. Also note that the truncated basis sets are quite different in size, which leads to different condition numbers for the isolated atoms.

For the sake of completeness, we also report the energy of a fcc He crystal at varying nearest-neighbor distances computed with our four basis sets. The potential curves along with the HF limit for the isolated He atoms are displayed in Fig. 3. Note that the more extensive (and more diffuse) basis sets allowed computations only for larger D, due to numerical linear dependencies which typically occurred when the smallest eigenvalue of **S(k)** dropped below 10^{-3} a.u.

All but the most truncated basis set yielded energies for the isolated He atoms which were just $7 \times 10^{-5}\,E_h$ higher than the HF limit. Only the smallest $(7s2p)/[3s2p]$ basis set, with the most diffuse primitive function being rather compact, led to an energy which was 4 mE_h above the HF limit. This basis also led to a bound region in the potential curve, with a dissociation energy of roughly

Table 1. Basis set for He[a]

l	$\alpha_i(a_0^{-2})$	c_i
s	799.861	0.0007087979
	113.852	0.0057978534
	25.5122	0.029432073
	7.27573	0.10662688
	2.40109	0.27193618
s	0.859007	1.0
s	0.324421	1.0
s	0.126636	1.0
s	0.0334228	1.0
s	0.0111537	1.0
p	1.73	1.0
p	0.58	1.0

[a] $E_{\text{tot}}(^1\text{S He}) = -2.861602E_h$

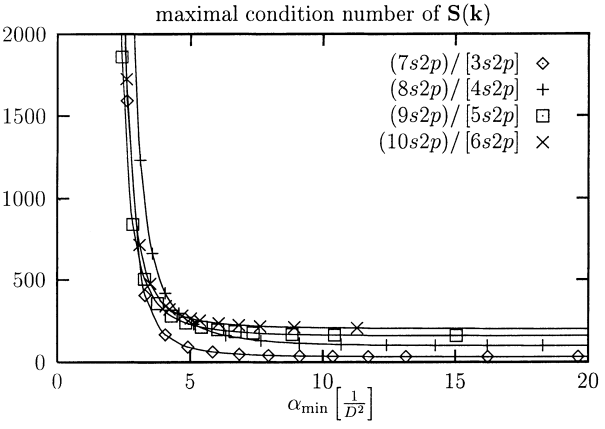

Fig. 2. Maximum condition number of the overlap matrix **S(k)** for a sample of 29 **k** points over the ratio of the smallest exponent of the basis set to the square of the nearest-neighbor distance

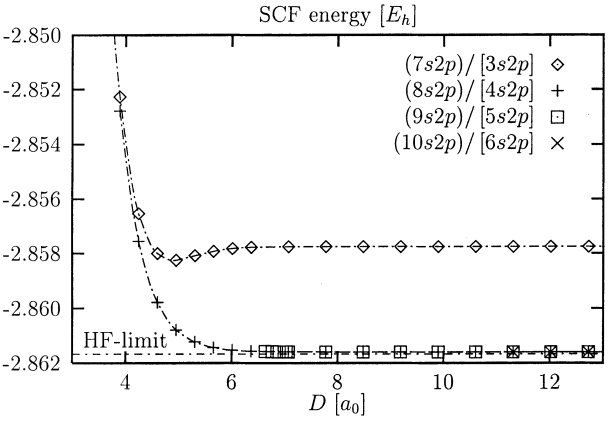

Fig. 3. Total *SCF energy* $[E_h]$ of a fcc He crystal for different nearest-neighbor distances D $[a_0]$

0.5 mE_h. At the HF-SCF level of theory this is clearly due to the BSSE. For smaller nearest-neighbor separations the energy difference between the smallest $(7s2p)/[3s2p]$ and the next larger $(8s2p)/[4s2p]$ basis set decreases from 4 mE_h for a nearest-neighbor distance of $D = 12.7\ a_0$ to about 0.5 mE_h for $D = 3.88\ a_0$. This result is expected [13], since atoms in a crystal can, to some extent, utilize the basis functions which are centered at their neighbors. One might be drawn to the conclusion that for a given basis set, the incompleteness error vanishes for more compact geometries of the crystal. This assumes, however, that higher angular momentum GTOs do not appreciably contribute to the energy of the crystal. Considering the ionization potential of He and its consequently small polarizability, this assumption seems fairly safe; for solids built from more easily polarized atoms like metals the situation might be very different though.

3.3 α-Beryllium

Hexagonal α Be was chosen as a test system, since with its relatively compact elementary cell, numerical linear dependency effects should be quite pronounced. With just four electrons per atom, only a relatively small number of basis functions should be required to reach the limit of a complete basis. Clearly, electron correlation is expected to be very different in Be atoms compared to the solid state, and HF-SCF theory cannot be expected to yield properties close to experimental results, but that is not our primary focus anyway.

An $(11s)/[7s]$ basis set was optimized for the Be atom, starting from an even-tempered set of exponents with $\gamma = 5$ and $\beta = 3$. γ was determined from a similar plot as Fig. 2, while T_Γ was taken as the experimental nearest-neighbor separation $D = 4.205\ a_0$ [21]. This corresponds to an absolute value of the pivot of $\alpha_{\min} = 0.2826\ a_0^{-2}$. The initial basis set was then extended by two auxiliary diffuse s-type GTOs, and subsequently optimized. The basis set obtained in this way was then contracted according to the scheme {5111111}. The two auxiliary primitives were then removed and polarization functions were added. The three p-type polarization functions were taken from the inner polarization contraction of Schäfer's TZP basis [22], while the two d-type exponents were set to 0.9 a_0^{-2} and 0.3 a_0^{-2} respectively. The final basis set as it was employed for the subsequent solid-state calculations is listed as vtz1 in Table 2.

The vtz2 basis set was derived from the vtz1 basis set by augmentation with two diffuse GTOs: one of s-type and one of p-type. The additional s-type exponent was optimized while the rest of the basis was kept fixed. Valence contractions were optimized, according to the scheme {51112/121/11}. For the s-type valence contraction this optimization was done for the atom, while the p-type contraction was optimized for a Be_2 "molecule" at a bond length of 4.2049 a_0. (This is the experimental nearest-neighbor distance in α-Be). The somewhat unconventional contraction pattern for the p-type basis was chosen to allow for an additional variational degree of freedom in the optimization of the wave function, which includes diffuse basis functions. This was deemed necessary since the population of the most diffuse p-type GTO as obtained from a Mulliken population analysis for α-Be using the vtz1 basis set was rather high (1.33) for the experimental geometry.

For both basis sets and for the extended basis set of Dovesi [16, 23], the energy as a function of nearest-neighbor distance was computed. To do so, the ratio of the two lattice constants was kept at the experimental value ($A/C = 0.63787$ [21]), while one axis A was varied. The potential curves obtained in this way are displayed in Fig. 4; the lattice constants A and C, total energies at the equilibrium geometry E_{tot}, and the virial ratio c_{vir} are listed in Table 3.

Both Dovesi's basis set and our vtz1 basis set describe the isolated Be atom rather poorly. This is a consequence of the smallest s-type exponent of both basis sets being rather large (0.27 a_0^{-2} and 0.245 a_0^{-2}, respectively). On the other hand, the vtz2 basis yields energies within 1 mE_h of the Hartree-Fock limit for the isolated atoms, due to a diffuse s-type function being included as a valence contraction.

Table 2. Basis sets for Be

l	$\alpha_i(a_0^{-2})$	vtz1[a] c_i	vtz2[b] c_i
s	6265.83	0.000444562	0.000444562
	1032.99	0.003076364	0.003076364
	240.280	0.016272378	0.016272378
	66.1461	0.069307201	0.069307201
	20.7578	0.22785662	0.22785662
s	7.17720	1.0	1.0
s	2.66819	1.0	1.0
s	1.04708	1.0	1.0
s	0.245751	1.0	0.36723142
	0.0716935	–	0.75904191
p	3.63298	1.0	1.0
p	0.713414	1.0	1.6398617
	0.102264	–	0.58719124
p	0.196089	1.0	1.0
d	0.9	1.0	1.0
d	0.3	1.0	1.0

[a] $E_{tot}(^1\text{S Be}) = -14.362253 E_h$
[b] $E_{tot}(^1\text{S Be}) = -14.571955 E_h$

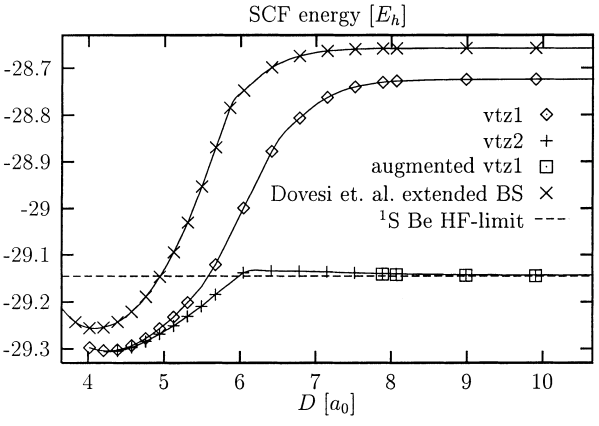

Fig. 4. Total *SCF energy* [E_h] of an α-Be crystal for varying nearest-neighbor distances D [a_0]

For the solid-state system we estimate that the energies computed with the vtz2 basis set are similarly close to the HF limit, since the inclusion of additional basis functions did not alter our results significantly. The effect of f-type GTOs (which are unavailable for the CRYSTAL 92 suite of programs) was probed by including s- and p-type GTOs located at the tetrahedral and octahedral interstices, which resulted in an energy lowering of less than 0.3 mE_h. Furthermore, including additional p- and d-type GTOs centered at the nuclei did not lower the calculated energies by more than 0.03 mE_h.

The most important difference between Dovesi's extended basis set and our vtz1 basis set lies in the fact that ours approaches the HF limit for the solid-state system, while that of Dovesi does not. An incomplete basis set should lead to compact geometries, due to the BSSE which generally results in underestimation of bond lengths [24], and to overestimation of the bulk modulus [18]. The situation is similar to restricted HF calculations on diatoms, which lead to overly small bond lengths and too high harmonic frequencies due to overestimation of the dissociation energy. Dovesi's basis set seems to both underestimate the bond length and to overestimate the curvature of the potential energy curve, while our basis sets in turn leads to overestimation of the bond lengths, presumably due to the neglect of electron correlation effects in HF-SCF theory.

Table 3. Lattice constants for α-Be obtained with different basis sets

	Basis set			
	Dovesi	vtz1	vtz2	Exp.
A (pm)	222.2	230.3	230.9	228.56
C (pm)	348.3	361.1	361.9	358.32
E_{tot} (E_h)	−29.2568	−29.3045	−29.3066	–
c_{vir}	1.0050	1.0003	1.0002	–

Another interesting feature of Fig. 4 is the barrier in the vtz2 potential curve at $D = 6.41\ a_0$, which is 9.2 mE_h higher than the energy for the isolated atoms. A similar maximum was observed in the SCF and CAS-SCF but not in the CI potentials of Be_3 in Ref. [25]. It can be attributed to SCF theory being unable to describe the dispersion (i.e., long-range attractive) terms of the total energy. This feature of SCF theory can only be reproduced if the basis contains sufficiently diffuse functions. The vtz1 basis set yields similar results (labeled "augmented vtz1") if it is augmented with two diffuse s-type GTOs ($\alpha = 0.102264, 0.041980\ a_0^{-2}$). For this augmented basis set, only a few points of the potential could be computed, since it produces near linear dependencies for $D < 7.8\ a_0$.

Our vtz1 and vtz2 basis sets not only yield essentially the same geometrical parameters but also a very similar electronic structure, which is in turn quite different from the one obtained with Dovesi's basis set. To illustrate this point, the differential density for the noninteracting atoms and the crystal was computed over the (1120) plane within one unit cell. Our approach was the same as in Ref. [23]. Figures 5 and 6 show the differential density obtained with the vtz2 and Dovesi's basis sets for the experimental equilibrium geometry (density in the crystal minus density of the noninteracting atoms). Positive values refer to an increase of the electronic density in the crystal. The vtz1 basis set yielded a differential density plot very similar to Fig. 5.

In general terms, there is an electron transfer from the core to the valence region of the atoms. This transfer is rather inhomogeneous, however, since there is an in-

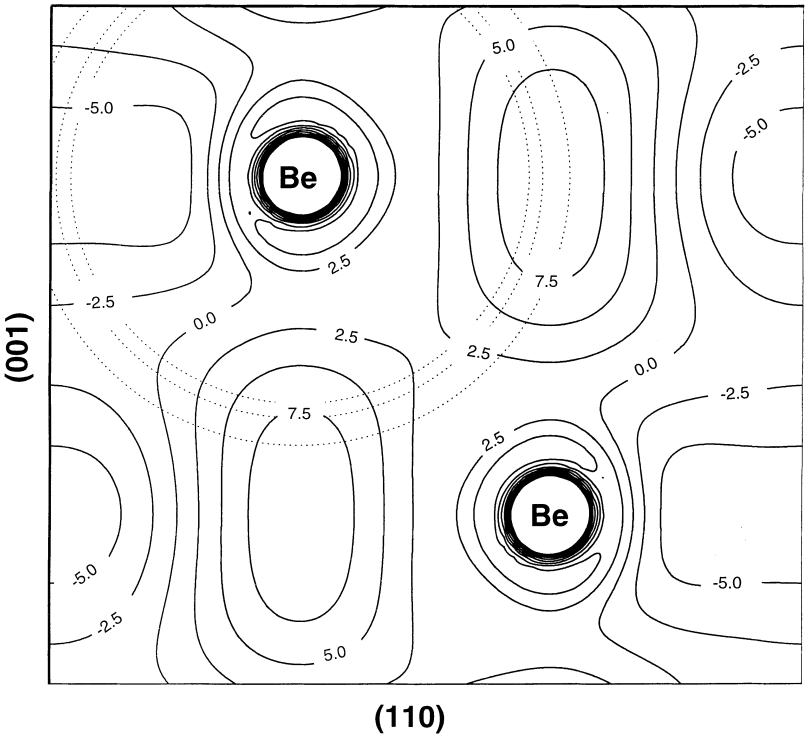

Fig. 5. Differential electronic density $(10^{-3} e a_0^{-3})$ of the noninteracting atoms and the crystal over the (1120) plane of the unit cell for the vtz2 basis. The *dotted circles* indicate the operator widths of Table 4

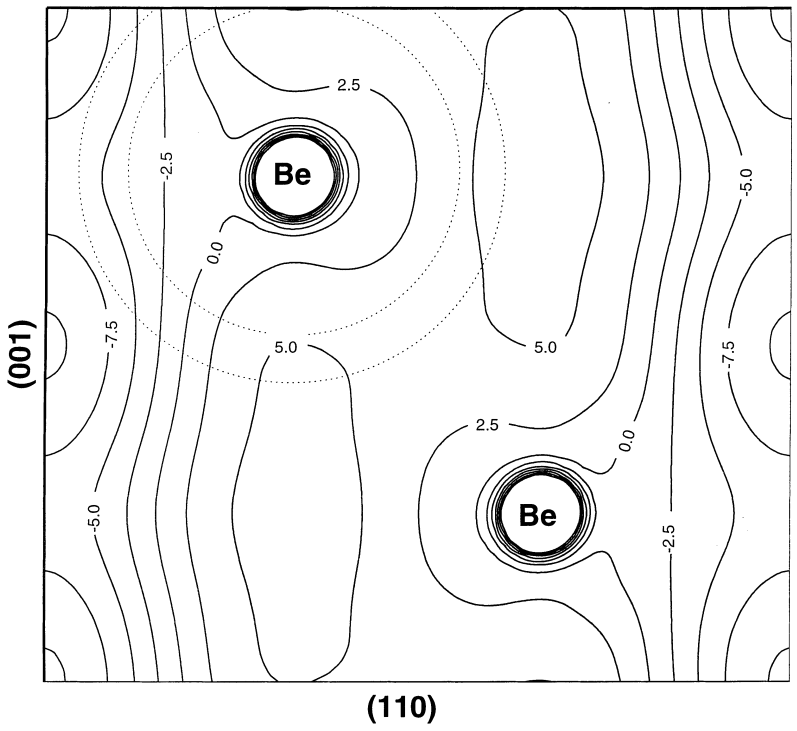

Fig. 6. Differential electronic density $(10^{-3}ea_0^{-3})$ of the non-interacting atoms and the crystal over the (1120) plane of the unit cell for Dovesi's basis set. The *dotted circles* indicate the operator widths of Table 4

Table 4. Operator widths $\Delta\hat{r}$ for the outermost basis functions for the vtz2 and Dovesi's basis sets

	$\Delta\hat{r}(a_0)$		
Type	*s*	*p*	*d*
vtz2	2.73	2.52	2.42
Dovesi	1.67	2.15	–

crease of electronic density in the tetrahedral and a decrease in the octahedral interstices. The first feature is much less pronounced for Dovesi's basis, (due to the lack of *d*-type GTOs), while the octahedral sites (at the corners of the plotted area and in the middle of its sides) are much more deprived of electronic density. This is due to Dovesi's basis set being more compact and hence less able to correctly describe the regions which are far away from (i.e., between) the nuclei.

The contraction pattern proposed above for the vtz2 basis set addresses precisely the features of the density within the unit cell which are present at the equilibrium geometry. Since additional functions in the contractions have small exponents, they mostly affect the tails of the orbitals and provide an enhanced operator width, $\Delta(\hat{r}) = \sqrt{\langle\hat{r}^2\rangle - \langle\hat{r}\rangle^2}$, for the outermost basis functions, as can be seen from Table 4. Conversely the lack of these (or similarly diffuse) functions will result in an inappropriate representation of the density at the interstices, as discussed above.

3.4 α-Boron nitride

In order to learn more about basis set effects in covalent solids we studied α-BN. Because of structural similarities α-BN is often referred to as inorganic graphite. Like graphite it has a sheet structure, with strong covalent bonding within the sheets and weak van-der-Waals-like bonding between them. Unlike graphite, the layers in α-BN are arranged in such a way that N positions in one sheet are matched with B positions in the neighboring sheets. Since one expects to find partial charges of opposite signs at the B and N centers, there should be some degree of electrostatic attraction between the sheets, which can be reproduced in the framework of HF-SCF theory. Even if dispersion forces between the layers are not present in the HF-SCF model, one might hope to recover at least a part of the bonding energy between them.

Two basis sets were optimized for α-BN. The first one, which we term "m-svp", is a modification of Dunning and Hay's split valence basis set [26][1]. It differs from the original basis set only in the exponents of the outermost primitive GTOs, which were first adjusted to circumvent numerical linear dependencies and then reoptimized with respect to the energy of a 2D layer of BN. The optimization led to a numerically linear dependent basis set in the third optimization cycle. Therefore, the results of the second cycle were used and are listed in Tables 5 and 6.

[1] The original basis set was obtained from the Extensible Computational Chemistry Environment Basis Set Database, version 1.0, as developed and distributed by the Molecular Science Computing Facility, Environmental and Molecular Sciences Laboratory which is part of the Pacific Northwest Laboratory, P.O. Box 999, Richland, Washington 99352, USA, and funded by the U.S. Department of Energy. The Pacific Northwest Laboratory is a multiprogram laboratory operated by Battelle Memorial Institute for the U.S. Department of Energy under contract DE-AC06-76RLO 1830. Contact David Feller, Karen Schuchardt, or Don Jones for further information.

The second basis set, which we term "tzp", was energy-optimized for the ^{2}P and ^{4}S states of B and N, respectively. The procedure adopted was the one described in Sect. 2.2. The pivots were chosen as $\gamma = 2/D^2 = 2/(2r_{\mathrm{cov}})^2$, where r_{cov} is the covalent radius of B (1.53 a_0) or N (1.32 a_0). In this case $\gamma = 2$ was chosen since hexagonal BN is not as densely packed as α-Be. The value of γ was determined from a similar plot as Fig. 2 for the structure of α-BN.

Both basis sets as well as one suggested by Causà [12] which we term CZ 6-21G*, were subsequently used to compute the equilibrium geometry of hexagonal BN. Causà's basis was derived from the well known 6-21G* series of basis sets [27] and reoptimized for use in a study on cubic BN. The lattice constants A and C, the total energies at the equilibrium geometry E_{tot}, and the virial ratio c_{vir} obtained with the three basis sets are listed in Table 7.

At first glance it seems the CZ 6-21G* basis set yields the best results for the geometry of the unit cell, despite the energy being far from optimal. This is, however, a spurious outcome, since the sheets of α-BN are not bound at all at the HF-SCF level of theory. This can be seen in Fig. 7, where the binding energies of the sheets per unit cell as a function of their separation are plotted. The potential curves labeled BSSE are the raw binding energies, defined as the difference between the energy of the unit cell at a given separation of the layers and of the isolated layers. The curves labeled CP have been corrected for the BSSE by the counterpoise method [29]. For this purpose, the energy of the isolated sheet was calculated with the basis functions of the two neighboring layers included. Clearly all basis sets result in purely repulsive potentials, which are in fact rather similar if the CP correction is applied. However, only our tzp basis set is able to describe the correct behavior of the potential curve even without correction, emphasizing that it is indeed close to the HF limit.

Table 5. Basis sets for N

l	N tzp[a]		N m-svp[b]	
	$\alpha_i(a_0^{-2})$	c_i	$\alpha_i(a_0^{-2})$	c_i
s	20527.6	0.003369005	5909	0.001190
	3077.30	0.026127932	887.5	0.009099
	699.427	0.13590992	204.7	0.044145
	197.779	0.54849282	59.84	0.150464
	64.4370	1.7413538	20.0	0.356741
			7.193	0.446533
			2.686	0.145603
s	23.1500	1.0	–	–
s	8.93684	1.0	–	–
s	3.58646	1.0	–	–
s	0.835485	1.0	7.193	−0.160405
			0.7	1.058215
s	0.285738	1.4133855	0.33	1.0
	0.0995290	0.23250588	–	–
p	74.3172	0.016550978	26.79	0.018254
	17.5273	0.11830121	5.956	0.116461
	5.45842	0.49223581	1.707	0.390178
	1.95578	1.3569285	0.5314	0.637102
p	0.74328	1.0	–	–
p	0.28574	1.3214430	0.2557	1.0
	0.10878	0.47610735	–	–
d	0.8	1.0	1.226859	1.0

[a] $E_{\mathrm{tot}}(^4\mathrm{S\ N}) = -54.346552E_h$
[b] $E_{\mathrm{tot}}(^4\mathrm{S\ N}) = -54.399978E_h$

Table 6. Basis sets for B

l	B tzp[a]		B m-svp[b]	
	$\alpha_i(a_0^{-2})$	c_i	$\alpha_i(a_0^{-2})$	c_i
s	13709.3	0.000568503	2788	0.001288
	2254.10	0.003876959	419	0.009835
	543.585	0.019275870	96.47	0.047648
	156.293	0.079560091	28.07	0.160069
	50.0927	0.27817595	9.376	0.362894
			3.406	0.433582
			1.306	0.140082
s	17.0606	1.0	–	–
s	6.03047	1.0	–	–
s	2.19062	1.0	–	–
s	0.499099	1.0	3.406	−0.17933
			0.3245	1.062594
s	0.217452	1.1837253	0.16225	1.0
	0.081605	0.75120640	–	–
p	73.4744	0.002244552	11.34	0.017988
	14.8716	0.021941253	2.436	0.110343
	4.25947	0.10364896	0.6836	0.383072
	1.46496	0.34157697	0.2134	0.647895
p	0.55969	1.0	–	–
p	0.218745	1.1529679	0.1267	1.0
	0.0762123	0.87382603	–	–
d	0.8	1.0	0.9	1.0

[a] $E_{\mathrm{tot}}(^2\mathrm{P\ B}) = -24.528568E_h$
[b] $E_{\mathrm{tot}}(^2\mathrm{P\ B}) = -24.507133E_h$

Table 7. Lattice constants, total energies, and virial ratios for hexagonal BN obtained with different basis sets

	Basis set			
	CZ 6-21G*	m-svp	tzp	Exp. [28]
A (pm)	250.3	248.8	249.4	250.4
C (pm)	664.3	681.2	891.0	666
E_{tot} (E_h)	−158.4356	−158.5592	−158.5895	–
c_{vir}	1.00016	1.00110	0.99996	–

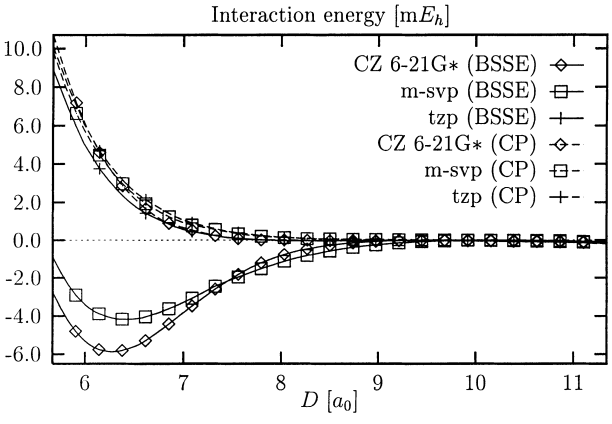

Fig. 7. *Interaction energy* [mE_h] of two BN layers at varying distances D [a_0] for different basis sets with and without counterpoise (*CP*) correction for the basis set superposition error (BSSE)

As in our study of α-Be, we simulated higher than *d*-type basis functions by including floating *s*- and *p*-type GTOs located midway between two atomic centers between the sheets. Doing so did not change any of the parameters computed with our tzp basis set significantly.

It is rather surprising indeed, that the sheets of α-BN are not bound at the HF level of theory. There is a sizable charge separation between the N and B centers, which according to Mulliken population analysis are roughly +1 and −1 respectively. Consequently one would expect α-BN to be at least somewhat bound by strong charge-charge electrostatic interactions of the neighboring centers. Obviously, Pauli repulsion outweighs this effect. This raises the question of whether the structures of other molecular solids can be correctly described at all with HF-SCF theory. After all, the interaction of higher than 0th-order multipoles decays much more rapidly than charge-charge interactions. For these reasons, the results of SCF theory for molecular crystals with structures that are not dominated by hydrogen bonding should be considered with great care. It should be noted that as in the case of α-Be, we found very little dependency of the occupied band structure on the choice of basis.

3.5 B1 Sodium fluoride

As a final example the B1 phase of sodium fluoride (NaF) was investigated. HF-SCF theory should be most successful for this test system. For ionic solids one expects the contribution of the correlation energy to be similar in the isolated ions and in the solid state, which results in a cancellation of errors. Two basis sets were energy-optimized with respect to the ground states of the constituent atoms (atom-tzp) and ions (ion-tzp) of NaF. The "ion-tzp" basis set was derived from complete optimization of uncontracted 11*s*7*p* (Na) and 12*s*7*p* (F) bases, which were subsequently contracted according to the scheme {611111/4111} (Na) and {6111111/4111} (F). Both the exponents and the contraction coefficients were optimized with respect to the energy of the ground-state ions. For the solid-state calculations a *d*-type polarization function was added to both basis sets. The final basis sets are listed in Tables 8 and 9.

The F^- and the Na^+ ions are quite compact, so it was found that no constraints with regard to the magnitude of the smallest exponents were necessary in the course of the optimization of the "ion-tzp" basis sets. Note that for this reason the most diffuse *p*-type exponent in the "ion-tzp" F basis turned out to be fairly small ($\alpha = 0.103487\ a_0^{-2}$). This should be compared to the exponent that Dunning suggested to augment his basis set for F^- ($\alpha = 0.074\ a_0^{-2}$) [26].

The "atom-tzp" basis sets were both optimized for the ground states of the respective atoms. A constraint in the optimization was only needed in the case of the *s*-type exponents of Na. A pivot was chosen as $5/(2r_{\text{ion}})^2 = 0.3365\ a_0^{-2}$, where r_{ion} is the ionic radius of the hexa-coordinated Na^+ ion (1.93 a_0). All other exponents were freely optimized and the resulting basis sets were then contracted according to the scheme {6111111/41111} (Na) and {6111111/31111} (F). The auxiliary *s*-type primitive (listed in parentheses in Table 8) of the "atom-tzp" set for Na was removed for the solid-state calculations and a *d*-type polarization function was added for F and Na. The basis sets employed for the solid-state calculations are listed in Tables 8 and 9.

The geometrical structure parameters were obtained via a fit of the energy of the conventional unit cell to Murnaghan's equation of state [30]:

Table 8. Basis set for Na

l	Na atom-tzp[a]		Na ion-tzp[b]	
	$\alpha_i(a_0^{-2})$	c_i	$\alpha_i(a_0^{-2})$	c_i
s	55476.6	0.000228374	47714.3	0.000268966
	8323.59	0.001766230	7769.56	0.001872322
	1897.11	0.009174810	1853.76	0.009294649
	537.085	0.037226367	540.917	0.036509024
	175.216	0.12010269	180.219	0.11597796
	63.1956	0.28910362	65.8824	0.27962557
s	24.4497	1.0	25.7375	1.0
s	9.77856	1.0	10.3771	1.0
s	2.60535	1.0	3.15371	1.0
s	0.949210	1.0	1.26011	1.0
s	0.336500	1.0	0.481033	1.0
s	(0.0413741)	1.0	–	–
p	538.245	0.000584429	268.973	0.001969871
	125.771	0.005047702	61.9061	0.016075204
	39.4588	0.026364155	19.3261	0.072913852
	14.2635	0.095741915	7.03621	0.20991428
p	5.60704	1.0	2.71150	1.0
p	2.25558	1.0	1.03283	1.0
p	0.889722	1.0	0.378912	1.0
p	0.334060	1.0	–	–
d	0.8	1.0	0.8	1.0

[a] $E_{\text{tot}}(^2\text{S Na}) = -161.85447 E_h$
[b] $E_{\text{tot}}(^1\text{S Na}) = -161.673463 E_h$

Table 9. Basis sets for F

l	F atom-tzp[a]		F ion-tzp[b]	
	$\alpha_i(a_0^{-2})$	c_i	$\alpha_i(a_0^{-2})$	c_i
s	65820.5	0.000151635	50421.6	0.000164812
	9907.62	0.001165934	7570.67	0.001289558
	2293.32	0.005883067	1704.96	0.006787004
	666.421	0.023572159	487.497	0.026866987
	221.040	0.079369264	165.147	0.083268106
	80.7903	0.21634446	63.5504	0.19818286
s	31.7082	1.0	26.9460	1.0
s	13.1269	1.0	12.1421	1.0
s	5.59238	1.0	5.49163	1.0
s	1.83029	1.0	1.70512	1.0
s	0.708778	1.0	0.635926	1.0
s	0.263666	1.0	0.215260	1.0
p	131.635	0.0036987415	112.063	0.003371059
	30.9968	0.027339404	26.7542	0.023839042
	9.76008	0.11478567	8.39446	0.098287601
	–	–	2.96677	0.25329800
p	3.53864	1.0	1.06294	1.0
p	1.343852	1.0	0.356540	1.0
p	0.500963	1.0	0.103487	1.0
p	0.177427	1.0	–	–
d	1.0	1.0	1.0	1.0

[a] $E_{\text{tot}}(^2\text{PF}) = -99.408301 E_h$
[b] $E_{\text{tot}}(^1\text{SF}^-) = -99.457559 E_h$

$$E(V) = E(V_0) + \frac{VB}{B'(B'-1)} \times \left\{ B' \left[1 - \left(\frac{V_0}{V} \right) \right] + \left(\frac{V_0}{V} \right)^{B'} - 1 \right\}. \quad (17)$$

For this purpose the lattice constant A was varied in the range 400–550 pm and the energy of the conventional cell was computed. Then the parameters in Eq. (17) were nonlinearly fitted to reproduce the computed energies. The parameters obtained in this way for the different basis sets are listed in Table 10.

As expected, the experimental values are reproduced rather well at this level of theory. Both the bulk modulus B and its first pressure derivative B' are computed within the limits of the corresponding experiments, and the equilibrium lattice constant deviates only slightly from it. The parameters computed with our "ion-tzp" basis set stand out somewhat from those computed with the other sets. This is a result of our "ion-tzp" basis set being somewhat more diffuse than the other basis sets which led to numerical linear dependencies for lattice constants smaller than 440 pm. For that reason fewer data points were available and hence the quality of the fitting procedure differed from that of the other basis sets. This can be seen from Fig. 8, where the individual points of the potential curves obtained with the three basis sets display very similar behavior, while the fitted energies differ considerably, particularly for small cell volumes. The structure parameters obtained with the basis set of Erikson et al. [18] differed somewhat from those derived in the original work of that group. We also attribute this to the different number of data points used in the iterative fitting procedure.

Despite our basis set yielding lower energies than that of Erikson et al. [18] we cannot add much to improve their analysis, to which we refer the interested reader instead. There is one point which needs to be stressed however. Erikson et al. optimized their basis sets for isolated ions and reoptimized the most diffuse exponents for the solid-state system. This procedure is only feasible for the fewest systems, since most isolated anions are unstable with respect to electron loss within the framework of HF theory. Our "atom-tzp" basis set in turn was optimized for the respective ground states of the isolated atoms and was used without further modification. The superior results obtained with this basis set

Table 10. Lattice constants A, bulk moduli B, first pressure derivative of the bulk modulus B', the total energies of the conventional cell of B1 NaF at the respective equilibrium geometries E_{tot}, and virial ratios c_{vir} obtained for different basis sets

	Erikson	Basis set		
		Atom-tzp	Ion-tzp	Exp.
A (pm)	462.8	463.1	462.2	463.4 ± 0.05
B (Mbar)	0.490	0.473	0.521	0.464 ± 0.062
B'	4.5	4.5	5.6	4.9 ± 1.2
E_{tot} (E_h)	−1045.918	−1045.926	−1045.923	–
c_{vir}	0.99991	0.99998	0.99998	–

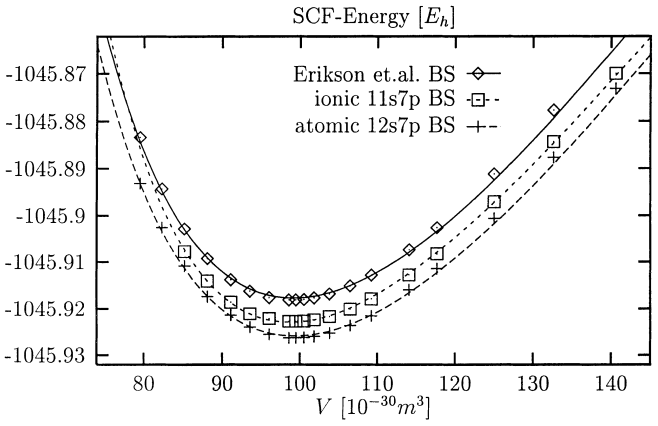

Fig. 8. Total energy of the conventional unit cell of NaF for varying cell volumes and different basis sets. The *points* correspond to computed energies, while the *lines* refer to the fitted energies

clearly demonstrate that costly reoptimization of a basis set for the solid state is not at all necessary, provided it is sufficiently extensive.

4 Conclusions

Several rules on how to optimize basis sets on isolated atoms for use in periodic HF-SCF calculations were derived. Utilizing these findings, new powerful basis sets were developed for the computation of a few representative solid-state systems. The subsequent calculations proved our basis sets to be generally superior to sets that are more limited but were reoptimized for the particular crystal at hand. In the case of α-Be and to a lesser degree in the case of α-BN we believe our results to be close to the complete basis set limit.

Furthermore, it was demonstrated how it is possible to include relatively diffuse functions into basis sets for periodic structures, thus improving the treatment of metals and of molecular crystals. In the case of metals such functions are necessary to correctly describe the free electrons in the crystal, while for molecular crystals diffuse functions are needed to reproduce nonbinding interactions. These nonbinding interactions were found to be dominant in the case of α-BN, which is not bound at the SCF level of theory. This poses the question of whether molecular crystals, which are often also dominated by nonbinding interactions, can be correctly descrcibed at this level of theory.

Acknowledgements. The authors wish to acknowledge the generous support of the Deutsche Forschungsgemeinschaft, which funded this work through SFB 334, Teilprojekt C7. Moreover, we acknowledge support by the Fonds der chemischen Industrie.

Reference

1. Helgaker T, Taylor PR (1995) In: Yarkony DR (ed) Modern electronic structure theory II. World Scientific, Singapore, pp 725–856
2. Davidson ER, Feller D (1986) Chem Rev 86: 681

3. Boys SF (1950) Proc R Soc London Ser A 200: 542
4. Schmidt MW, Ruedenberg K (1979) J Chem Phys 71: 3951
5. Almlöf J, Taylor PR (1987) J Chem Phys 86: 4070
6. Halkier A, Koch H, Jørgensen P, Christiansen O, Beck Nielsen IM, Helgaker T (1997) Theor Chim Acta 97: 150
7. Klahn B (1985) J Chem Phys 83: 5749
8. Klahn B (1985) J Chem Phys 83: 5754
9. Kutzelnigg W (1994) Int J Quantum Chem 51: 447
10. Starikov EB (1996) Int J Quantum Chem 57: 851
11. Ruiz E, Alvarez S, Alemany P (1994) Int J Quantum Chem 52: 365
12. Causà M, Zupan A (1994) Chem Phys Lett 220: 145
13. Pisani C, Dovesi R, Roetti C (1988) Hartree-Fock ab initio treatment of crystalline systems. Springer, Berlin Heidelberg New York
14. Dovesi R, Ermondi C, Ferrero E, Pisani C, Roetti C (1984) Phys Rev B 29: 3591
15. Causà M, Dovesi R, Pisani C, Roetti C (1986) Phys Rev B 33: 1308
16. Pisani C, Aprà E, Causà M, Orlando R (1990) Int J Quantum Chem 38: 419
17. Nada R, Nicholas JB, McCarthy MI, Hess CA (1996) Int J Quantum Chem 60: 809
18. Erikson RL, Eary E, Hostetler CJ (1993) J Chem Phys 99: 336
19. Surrat GT, Euwema RN, White DL (1976) Phys Rev B 8: 4019
20. Dovesi R, Saunders VR, Roetti C (1992) CRYSTAL 92 an ab initio Hartree-Fock LCAO program for periodic systems, user manual
21. Macgillavry CH, Rieck GD, Lonsdale K (Eds) (1968) International tables for X-ray crystallography, vol. III. Kynoch Press, Birmingham
22. Schäfer A, Horn H, Ahlrichs R (1992) J Chem Phys 97: 2571
23. Dovesi R, Pisani C, Rica F, Roetti C (1982) Phys Rev B 25: 3731
24. Dujineveldt FD, Dujineveldt-van de Rijdt JGCMC, Lenthe J.H. van (1994) Chem Rev 94: 1873
25. Harrison RJ, Handy NC (1986) Chem Phys Lett 123: 321
26. Dunning TH Jr, Hay PJ, (1997) In: Schaefer HF III (ed) Methods of electronic structure theory, vol 2. S. Plenum Press, New York
27. Gordon MS, Binkley JS, Pople JA, Hehre WJ (1982) J Am Chem Soc 104: 2797
28. Pease RS (1952) Acta Crystallogr 5: 356
29. Boys SF, Bernardi F (1970) Mol Phys 19: 553
30. Murnaghan FD (1944) Proc Natl Acad Sci USA 30: 244